RCEX: Rip Current Experiment

Jamie MacMahan & Ad Reniers
Oceanography Department, Spanagel 327c, Naval Postgraduate School, Monterey, CA 93943
Phone: (831) 656-2379   Fax: (831) 656-2712   Email: jhmacmah@nps.edu

NPS Award Number: (N0001407WR20226, N0001408WR20157)

Applied Marine Physics department, Rosenstiel School of Marine and Atmospheric Science,
University of Miami, Miami, Fl, 33149
Phone: (305) 421-4223   Fax: (305)   Email: areniers@rsmas.miami.edu

RSMAS Award Number: (N000140710556)

LONG-TERM GOALS

The long-term goals are to understand surf zone processes related to rip current systems through field observations. Rip currents occur commonly on most beaches and dominate many. It is recognized that beaches with straight and parallel contours are not a stable morphologic configuration whereas more complex beaches, which support the existence of rip current morphology, are stable and more common.

OBJECTIVES

The research objectives of the proposed work focus on obtaining new observations of the three-dimensional structure of the rip current system utilizing a suite of *in situ* instruments. In addition, a fleet of 30 inexpensive surfzone drifters were constructed and deployed to evaluate Lagrangian rip current associated observations. The second related effort applies a numerical model (Delft3D) to evaluate the dynamics of the rip current system and its interaction with the surface wave field and bottom topography. These new observations will be used to validate Delft3D and extend our understanding of rip current processes.

APPROACH

We (MacMahan, Stanton, Reniers, Thornton, Gallagher, Brown, Brown, Henriquez, Stockel, Cowen, Wycoff, and Morrison) conducted a Rip Current EXperiment, RCEX, at Sand City, Monterey Bay, CA in April-May 2007. A combination of *in situ* Eulerian measurements, remote sensing techniques, and Lagrangian measurements were deployed. The Eulerian measurements consisted of two primary arrays: 1) a cross-shore array of co-located pressure and digital electromagnetic current meters (PUV) and ADCPs along the axis of the rip channel, and 2) an alongshore array of PUVs and Paroscientific pressure sensors (PARO; Figure 1). The two-axis current and pressure PUV sensors provide data for analyzing alongshore wavenumber-frequency spectra, and a cross-shore array of bottom-mounted ADCP's captures the cross-shore variability in vertical flow structure within a rip channel. Remote sensing systems consisted of video and HF radar.

Report Documentation Page		*Form Approved* *OMB No. 0704-0188*

Public reporting burden for the collection of information is estimated to average 1 hour per response, including the time for reviewing instructions, searching existing data sources, gathering and maintaining the data needed, and completing and reviewing the collection of information. Send comments regarding this burden estimate or any other aspect of this collection of information, including suggestions for reducing this burden, to Washington Headquarters Services, Directorate for Information Operations and Reports, 1215 Jefferson Davis Highway, Suite 1204, Arlington VA 22202-4302. Respondents should be aware that notwithstanding any other provision of law, no person shall be subject to a penalty for failing to comply with a collection of information if it does not display a currently valid OMB control number.

1. REPORT DATE **2008**	2. REPORT TYPE	3. DATES COVERED **00-00-2008 to 00-00-2008**

4. TITLE AND SUBTITLE **RCEX: Rip Current Experiment**	5a. CONTRACT NUMBER
	5b. GRANT NUMBER
	5c. PROGRAM ELEMENT NUMBER
6. AUTHOR(S)	5d. PROJECT NUMBER
	5e. TASK NUMBER
	5f. WORK UNIT NUMBER

7. PERFORMING ORGANIZATION NAME(S) AND ADDRESS(ES) **Naval Postgraduate School,Oceanography Department,Spanagel 327c,Monterey,CA,93943**	8. PERFORMING ORGANIZATION REPORT NUMBER

9. SPONSORING/MONITORING AGENCY NAME(S) AND ADDRESS(ES)	10. SPONSOR/MONITOR'S ACRONYM(S)
	11. SPONSOR/MONITOR'S REPORT NUMBER(S)

12. DISTRIBUTION/AVAILABILITY STATEMENT **Approved for public release; distribution unlimited**

13. SUPPLEMENTARY NOTES

14. ABSTRACT

15. SUBJECT TERMS

16. SECURITY CLASSIFICATION OF:			17. LIMITATION OF ABSTRACT	18. NUMBER OF PAGES	19a. NAME OF RESPONSIBLE PERSON
a. REPORT **unclassified**	b. ABSTRACT **unclassified**	c. THIS PAGE **unclassified**	**Same as Report (SAR)**	**15**	

30 surfzone drifters with accurate GPS-tracking were deployed for three hours for seven different days under varying wave and tidal conditions to quantify the spatial variation in mean Lagrangian flow, dispersion, and diffusion. The GPSs after post-processing have an absolute position error of < 0.3 *m* and speed errors of < 3 *cm/s* (MacMahan et al., 2008). High resolution velocity measurements over large area are required to map the complete cell circulation of rip currents.

Concurrent numerical model predictions of the local hydrodynamic conditions were performed to help in the deployment of the surfzone drifters and the execution of jet-ski surveys. These computations are based on the transformation of deep water directional spectra to the nearshore, including the wave groups to simulate the three dimensional infragravity time scale surfzone circulations.

Jeff Brown (University of Delaware graduate student), Rob Wyland (NPS tech), Ron Cowen (NPS tech), Jim Lambert (NPS Tech), Jon Morrison (NPS student), Jamie MacMahan (NPS) constructed the surfzone drifters. MacMahan, Stanton, Reniers (RSMAS), Thornton(NPS), Gallagher (Franklin and Marshall), Brown, Brown, Henriquez (Delft), Stockel (NPS tech), Cowen, Wycoff (NPS tech), and Morrison were responsible for instrument deployment, maintenance, data archiving, removal, drifter depoyments, and bathymetric surveys. Currently, there are 5 students utilizing the dataset for Masters thesis. Two students (Jeff Brown and Jenna Brown) are from the University of Delaware and three students (Jon Morrison, and Andrea O'Neil) from the Naval Postgraduate School. In addition Martijn Henriquez (University of Delft) will use the data obtained from the near bed observations of velocity and sediment fluxes as part for his PhD thesis to examine intra-wave sediment transport processes.

WORK COMPLETED

We successfully deployed an alongshore array of PUVs and a cross-shore of ADCPs within a rip channel. We performed 7 drifter deployments under various wave, tidal, and surfzone flow conditions. We performed 5 bathymetric surveys over the course of the experiment. Delft3D has been coupled to the global wave model Wavewatch III, where the freq. directional spectra from Wavewatch III are used as input to the embedded SWAN model within Delft3D to calculate the transformation of deep water wave conditions to the nearshore zone. The SWAN-derived nearshore wave conditions were subsequently used as input for the wave group modeling suite within Delft3D resulting in predictions of the three dimensional surfzone circulation patterns on the infragravity time scales and longer. Next the combined three dimensional Lagrangian/Eulerian flow field was extracted from the Delft3D flow computations and used to predict the dispersion of surfzone drifters. The GPS-drifter observations have been analyzed to yields estimates of surfzone diffusion and dispersions using two-particle and cluster statistics. Post-experiment modeling has been performed to verify modeling concepts and numerical implementations in Delft3D, using the observed frequency directional spectra at 12.8 m water depth to construct the offshore wave boundary (Reniers et al., 2008) and compare with GPS-drifter inferred surface velocities and Eulerian in situ measured sub-surface velocities.

RESULTS

The experiment was highly successful in providing many necessary observations for evaluating rip current dynamics.

Lagrangian Observations

The rectified time-averaged breaking wave patterns for four representative drifter observation patterns are plotted in Figure 1 (left column). Drifter observations are subdivided into three primary flow patterns: 1) symmetric and asymmetric rip currents that were observed when $H_{mo,13m} > 1$ m, 2) wandering currents that was a combination of rip current flow pattern and sinuous alongshore flow pattern that were observed when $H_{mo,13m} \geq 1$m, and 3) sinuous alongshore currents that were observed when $H_{mo,13m} < 1$m.

For the first time, a synoptic circulation pattern of a rip current is observed in the field with enough resolution to calculate the vorticity field (Figure 2a,b). Two different rip current circulation patterns were observed: 1) symmetric rip current circulation (Figure 2a) and 2) asymmetric rip current circulation (Figure 2b). The symmetric rip current has onshore flows over the shore-connected shoals that transition to alongshore flows (feeder currents) near the shoreline which converge and move offshore in the rip channel, and transition to alongshore flows that diverge near the surf zone edge inducing a counter (positive vorticity)- and a clockwise (negative vorticity) rotational element (rip current vortex). These two opposing rotational elements are a rip current system that is generally bounded in the cross-shore by the surfzone width and in the alongshore by the "quasi" alongshore periodic rip channels. The faster velocities occur near the outer edges of the rotational elements, with the slowest velocities occurring near the vortex centers. Asymmetric rip currents are similar to symmetric rip currents, except that the vortex occupies one rip channel and one shore-connected shoal and has up- or down coast preference. Areas of opposing vorticity occur near the edges of adjacent rip current cells. Maximum absolute vorticity occurs in the center of the rip current cells. The rip current pattern and surfzone vorticity estimates are consistent with numerical model estimates [Reniers et al., 2007; amongst others].

Lagrangian rip current circulation patterns are quantitatively documented in the field for the first time. These Lagrangian observations provide useful insights about the behavior of rip currents and surfzone exchange. Surprisingly, the rip current flow field consisted of semi-enclosed vortices that retained material within the vortex center and were contained within the surf zone. The drifter observations increase toward the center of the rip current vortices for energetic conditions when the circulation pattern is coherently organized. Talbot and Bate [1987] found surfzone diatom blooms were correlated with larger breaking waves and rip current events, and the largest concentrations of surfzone diatoms were toward the center of rip current vortices. Our drifter results support their findings and indicate that despite the large velocities in the rip channel; diatoms, pollution, and other floatsom are not necessarily transported offshore but are instead retained and concentrated within the rip current vortices inside of the surf zone. Unlike ocean vortices that trap and transport material, the rip current vortex is fixed in one location, as it is coupled to the surfzone morphology, and only retains the material and does not transport it.

The observed semi-enclosed surf zone circulation patterns have significant importance to Navy personnel with regard to beach safety. For most rip current drifter deployments, swimmers were often caught in the rip current while releasing the drifters. Swimmers would float and ride the circulation pattern back to wading depths on the shore-connected shoal, mimicking the drifter response. The drifters can be considered proxies for floating humans. For the asymmetric rip current day, GPSs were placed on a few swimmers as they freely floated in the rip current system. An example of one person who floated around a rip current for two revolutions is shown in Figure 2. The average swimmer

3

revolution was approximately 7 minutes, similar to average drifter revolution [Brown et al., 2008] and dye revolutions [MacMahan et al., 2008]. In general, beach-goers are told to "swim parallel" or along the shoreline when pulled into a rip current (www.usla.org). The alongshore currents feeding the rip current can be as large as the rip current (Figure 2). These results suggest that if the swimmer remains calm and afloat, they will be returned to wading depths in less than three minutes. However, there are times, though infrequent 10%, that they may exit the surf zone. No swimmer exited the surf zone during the experiment.
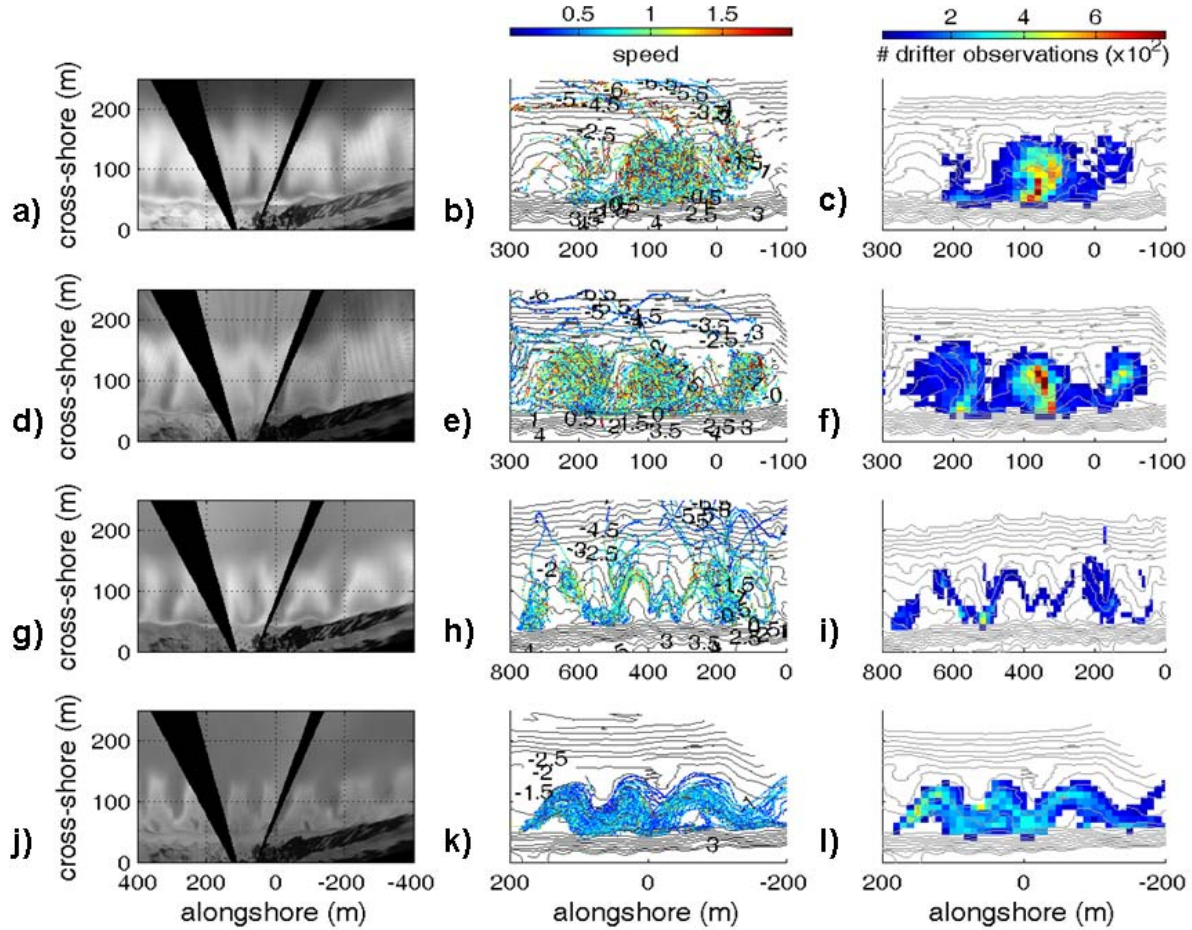

Figure 1. left column) Three video cameras overlooking the experiment site were mounted on a tower 18.2 m above the mean sea level. (middle column) Drifter position and speed (colorline) tracks for the four representative flow patterns. The colorbar at the top represents drifter speed. (right column) For drifter observations described herein, the biases in sample density and temporal intervals [Davis, 1991]

Swenson and Niiler, 1996] are minimized, as drifters repeatedly looped around a rip current rotational element and/or drifters were repeatedly re-released providing temporally-evolving iterative observations in space. Owing to these factors, each drifter was considered an independent observation when in a particular defined binned area. If the drifter re-entered the same area, it was considered a new independent observation, but only for $t > lg/U$ has elapsed, where lg is the length of the bin and U is the average speed in the box for all drifter observations. Five independent observations are

considered as statistically reliable [Spydell et al., 2007]. Bathymetric contours are plotted in the background in gray. Colorbar at the top represents the number drifter observations for 10m by 10m bins with greater than four independent observations.

Surfzone Dispersion and Diffusivity on a Rip Channeled Beach

Absolute and relative diffusivity are computed within the surf zone using 30 position-tracking drifters released in clusters (4 - 12 drifters) deployed on 7 days with different wave forcing and tidal elevations on a sandy beach with quasi-periodic alongshore spaced, O(125 m), rip channels (currents) at Sand City, Monterey Bay, CA. Diffusivity and dispersion were found to be larger on days with rip current flow patterns and larger waves and are comparable to previous surf zone estimates at the asymptotic limit. The cross-shore absolute diffusivity κ_{xx} asymptotes measured here (0.9 - 2.2 m^2/s) on days with rip current flow patterns are similar in magnitude to earlier dye measurements on a beach with rip currents (0.08 - 5.9 m^2/s), but alongshore absolute diffusivities measured here (2.8 - 3.9 m^2/s) are an order of magnitude larger than the 0.03 - 0.2 m^2/s measured by Inman et al., [1971]. Absolute diffusion in the rip current flow patterns is initially dominated by the cross-shore, as found by Inman et al. [1971], but for large *t* the diffusion becomes alongshore dominated similar to Johnson and Pattiaratchi [2004]. The large initial diffusivity followed by a sharp decline results from the expansion and contraction, as the particles are quickly dispersed initially then begin to re-group, slowing the spread. The rip current causes material to diffuse quickly for *t*<90 s in the cross-shore (κ_{xx} = 4.9 - 6.1 m^2/s), before decreasing to an asymptotic oscillation (κ_{xx} = 0.9 - 2.2 m^2/s), while alongshore material diffusion is initially (*t*<170 s) smaller than cross-shore diffusion and asymptotes at a larger value (κ_{yy} = 2.8 - 3.9 m^2/s). The cross- and alongshore absolute diffusivity modulates at ~300 s corresponding to the average circulation time for a rip current. For the sinuous alongshore flow field, which more closely represents the conditions observed by Spydell et al. [2007], the alongshore diffusivities measured here are similar in magnitude (2.4 - 2.7 m^2/s) to theirs (2.0 - 4.5 m^2/s). Initial cross-shore diffusivities for the alongshore current systems (2.6 - 3.7 m^2/s) are larger than those observed by Spydell et al. [2007] (0.7 - 1.5 m^2/s) though they decrease to more comparable values at later times (0.1 - 2.5). On days exhibiting the same flow pattern, absolute diffusivities are smaller for days with smaller waves and shorter periods, resembling Spydell et al. [2007], though the exact relationship between flow pattern, wave conditions and diffusivity cannot be generalized due to the lack of data. The cross-shore diffusivity on yearday 139 exemplifies the difference bathymetric variations and flow pattern can make on the diffusivity. Wave heights and period are similar to day 1 of Spydell et al. [2007], but the sinuous alongshore flow restricts particle dispersion to the surf zone and the cross-shore diffusivity falls to zero, while for Spydell et al. [2007] the cross-shore diffusivity reaches a non-zero asymptote.
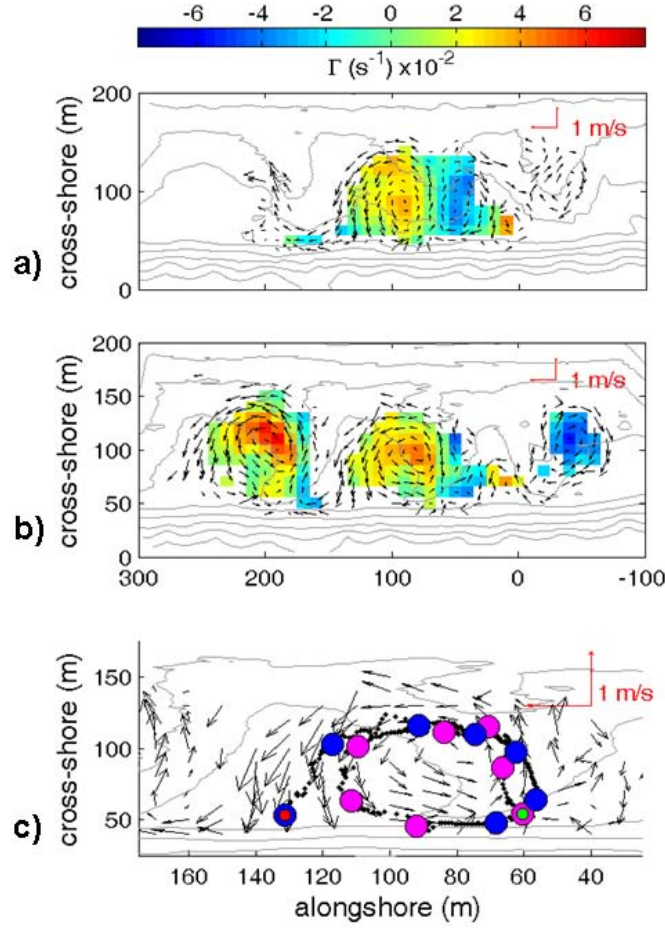
Figure 2. a,b) Rip current velocity data are sorted into 10m by 10m bins and averaged over the deployment duration (~3 hours) for that day for bins with greater than four independent observations (Figure 1, right column). The red arrows in the upper right-hand corner provide vector scales. The local bottom morphology is contoured in the background. Vorticity is calculated in discrete form using a weighted central difference method and plotted behind the velocity vectors (left column - a,b). Note since bin quantity is computed from nine bins surrounding the center bin, there are a small number of observations that occur without a velocity observation within that center bin. Owing to the statistical uncertainity of the spatially-weighted central-difference kinematic estimate, a Monte Carlo simulation is performed using the spatial mean velocity field and randomizing the velocity standard deviation for each grid cell. The mean standard deviation for Monte Carlo simulations is 0.019s^{-1}, which we consider as our error. The hot and cold vorticity estimates are generally larger than the error. c) The circles on the dotted line represent minutes starting at zero (green) and ending at 14 (red) for the human drifter track. Two revolutions of human track are plotted (magenta for the 1st revolution and blue for the 2nd revolution). The local bottom morphology is contoured in the background.

Battjes [1975], assuming straight and parallel contours used an energy balance ($\dfrac{dEc_{gx}}{dx} = \varepsilon_b$) to solve for the turbulent eddy diffusion by assuming the production of turbulence generated is locally equal to

dissipation by breaking waves, ε_b, where E is wave energy and the group velocity in the x direction $c_{gx} \approx c_g$ for the assumed normally incident waves. The turbulent eddy viscosity given by:

$$\upsilon_t = \alpha H \left(\frac{\varepsilon_b}{\rho} \right)^{1/3}$$

(1)

where ρ is density of seawater, with the scale of the turbulence given by H, the incident wave height representing a mixing length and α a calibration factor of O(1). Neglecting wave reflection or transfer to lower frequency waves, all incident wave energy is dissipated by wave breaking within the surfzone, and the surf zone-averaged wave energy dissipation, $\bar{\varepsilon}_b$, can be obtained from the wave energy balance by integrating over the surfzone width, X_S, yielding:

$$\bar{\varepsilon}_b = \frac{1}{X_S} \int_0^{X_S} \frac{dEc_g}{dx} dx = \frac{(Ec_g)_{X_S} - (Ec_g)_0}{X_S}$$

(2)

Outside the surf zone, the incident energy flux is constant and can therefore be evaluated with the measurements obtained at 13 m depth (Table 1) whereas the energy flux at the shore line, $x = X_S$, equals zero. Hence, the surfzone averaged wave energy dissipation is calculated :

$$\bar{\varepsilon}_b = \frac{\left(Ec_g\right)_{x|h=-13m}}{X_s}$$

(3)

with the incident wave energy given by:

$$E = \frac{1}{16} \rho g H_s^2$$

(4)

and the group velocity obtained from linear wave theory:

$$c_g = \left(\frac{1}{2} + \frac{kh}{\sinh(2kh)} \right) \frac{\omega}{k}$$

(5)

where $\omega = \frac{2\pi}{T_p}$ with T_p as the period of the peak of the wave spectrum and the wave length k is obtained from the linear dispersion relation:

$$\omega^2 = gk \tanh kh$$

(6)

The cluster-drifter based analysis of the turbulent eddy diffusivity, k_{xy}, represents a surf zone-averaged quantity (90% of the drifters stay within the surfzone). Using the values for waves in 13 m water depth and an optimized constant value of $\alpha = 0.7$ and X_S to 125 m, there is a significant correlation between the estimated surfzone averaged wave-breaking induced turbulent eddy viscosity, υ_t, and the estimated turbulent eddy diffusivity k_{xy} at the 95% confidence interval ($R^2 = 0.95$).
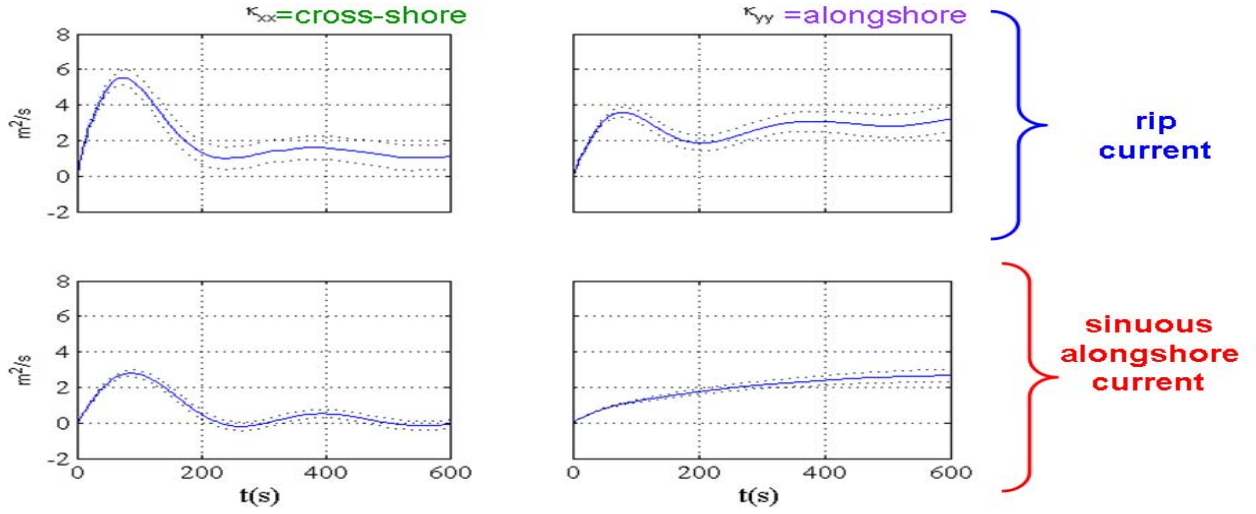
7

Figure 3. absolute diffusivity (one-particle) statistics (κ_{xx} (left) κ_{yy} (right) plotted with sampling error bars δ(t) [dotted lines] against time for yeardays 124 (top row) and 139 (bottom row). Peaks in κ_{xx} occur at increments of ~300 s corresponding to the oscillations in the auto-covariance functions and the circulation times of the rip circulation cells [MacMahan et al. 2008a]. The quick growth of κ_{xx} for t'<100 s followed by a sharp decrease is reflected in early rapid growth in σ_{xx} followed by slower expansion. At the time of the initial peak in κ_{xx}, the cross-shore patch size σ_{xx} ≈ 25 m, indicating that for a basically Gaussian distribution, 96% of the drifters are contained within $4\sigma_{xx}$ ≈ 100 m, roughly the cross-shore rip current dimension (within 15% difference), indicating the particles diffuse quickly until they span the entire surf zone at which time cross-shore diffusivity slows as particles oscillate between the seaward edge of the surf zone and the shoreline [MacMahan et al., 2008a]. On yearday 139 the cross-shore absolute diffusivity, κ_{xx}, peaks at 2.8 m^2/s then drops to near zero as cross-shore patch expansion stops almost completely after the initial dispersion. The difference in diffusivity is associated with the difference in the flow patterns.

Delft3D Model Calculations

A 3D wave and flow model (Delft3D) has been used to compute the wave and velocity field at the wave-group time scale. Comparison with *in-situ* ADCP measurements show that the hourly-mean variation is qualitatively well represented (Figure 4). Important differences do occur, most notably in the prediction of the vertical structure of the rip current flow outside the outer surf zone where the observed strong vertical attenuation is not present in the computations.
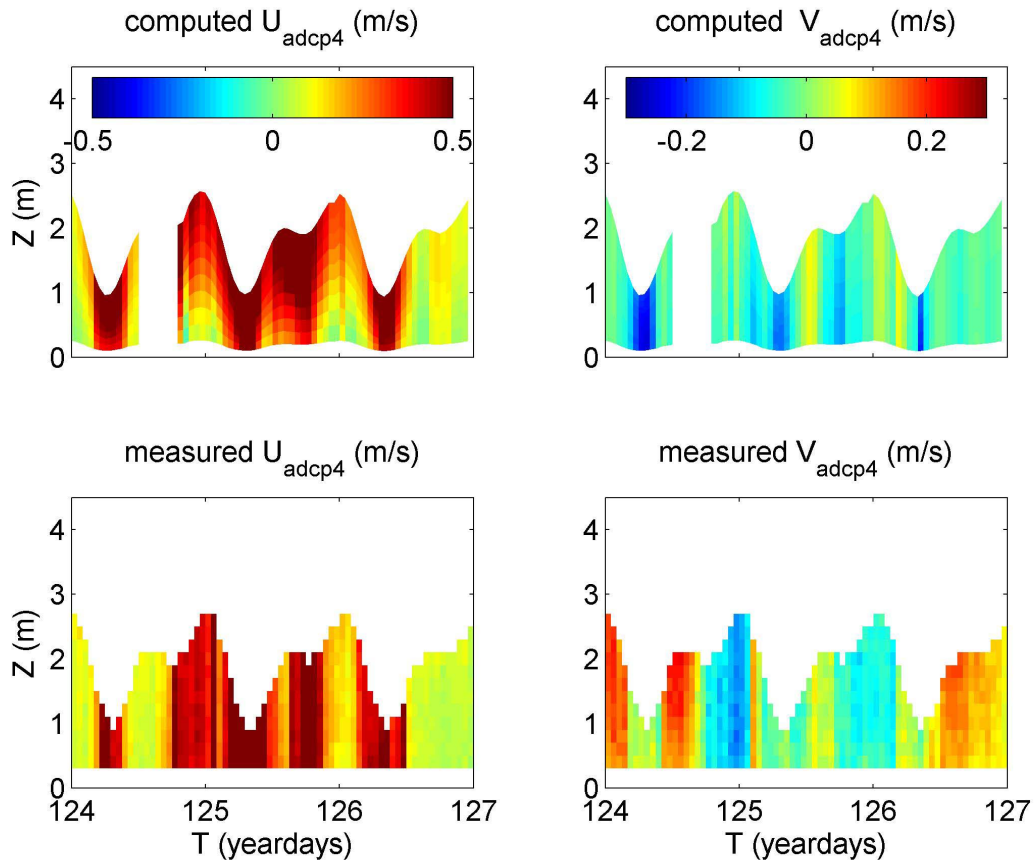
Figure 4 Hourly mean flow velocity at ADCP4 (outer surfzone). Upper panels computed cross-shore (left) and alongshore (right) Eulerian velocity (positive offshore and downcoast). Lower panels: similar for observed velocities.
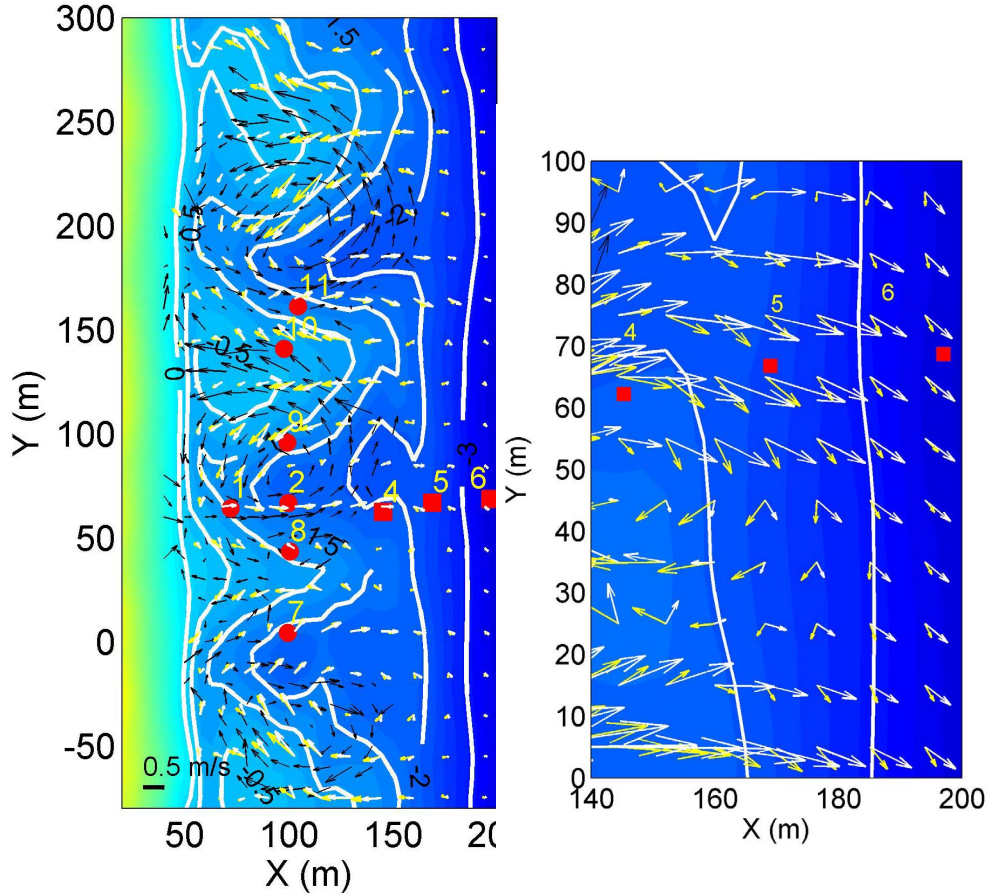
Figure 5 Left panel: GPS-inferred mean velocities for the deployment on yearday 124 compared with computed mean surface velocities including Stokes drift (GLM-velocities indicated in yellow) and without (Eulerian velocities indicated in white). Middle panel: Detailed view of both GLM and Eulerian mean surface flow velocities showing the stronger curvature for the GLM velocities.

Averaging the wave-group resolving surface velocities over the duration of the drifter deployment on yearday 124 yields the mean surface velocity field which is compared with the GPS-drifter inferred velocities (Figure 5). The computations show similar flow circulations as the observations with onshore velocities over the shallow shoals feeding into the rip currents. Details on the flow divergence and convergence of the asymmetric flow circulations are also well represented. The offshore extend of the rips is limited due to the fact that the offshore flow quickly diverges resulting in mean vortical circulations. The GLM (including Stokes drift) and Eulerian (without Stokes drift) mean flow velocities are very similar in a qualitative sense (Figure 5). However, a detailed look of the flow velocities at the outer surf zone shows that the Eulerian flow field generally has stronger offshore directed velocities in the rip channels (right panel in Figure 5). The alongshore velocity are only moderately affected and as a result the GLM velocities exhibit a stronger rotation (i.e. smaller radius) compared with the Eulerian velocities.
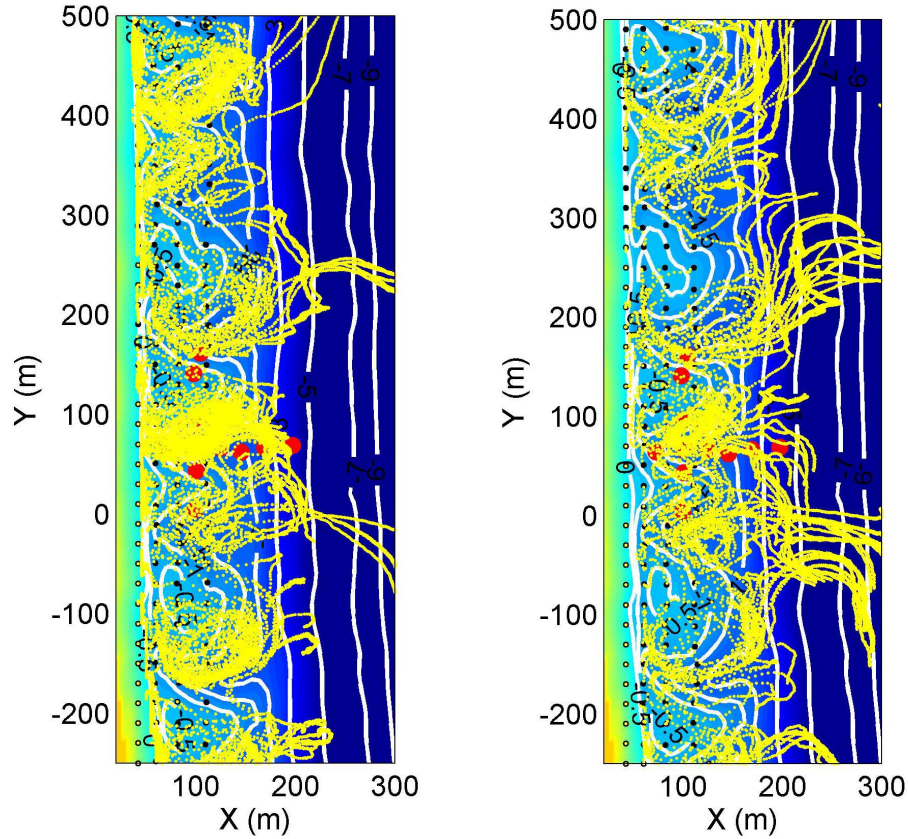
Figure 6 Left panel: Initial drifter locations (black circles) and calculated trajectories (yellow dots) using the GLM velocities for yearday 124 for hour 10. Right panel: Similar for Eulerian velocities. Position of the outer surfzone edge is indicated by red dashed line. Bathymetry and depth contours in m given as a reference.

The calculated surface velocity fields, at the wave group time scale, are used to predict the trajectories of virtual surface drifters. This is done for GLM velocities (including Stokes drift) and Eulerian velocities (without Stokes drift) (Figure 6), where the latter result generally in a nearcomplete exodus of the drifters within the hour. Using the GLM velocities the majority of the drifters are still within the surf zone after one hour. This is a result of the fact that the GLM velocities exhibit a stronger rotation compared with the Eulerian velocities (Figure 5). The GLM derived results are consistent with the field observations, whereas the Eulerian results over-predict the number of drifter exits by an order of magnitude. This stresses the importance of including Stokes drift in calculating the transport of surface floating material.
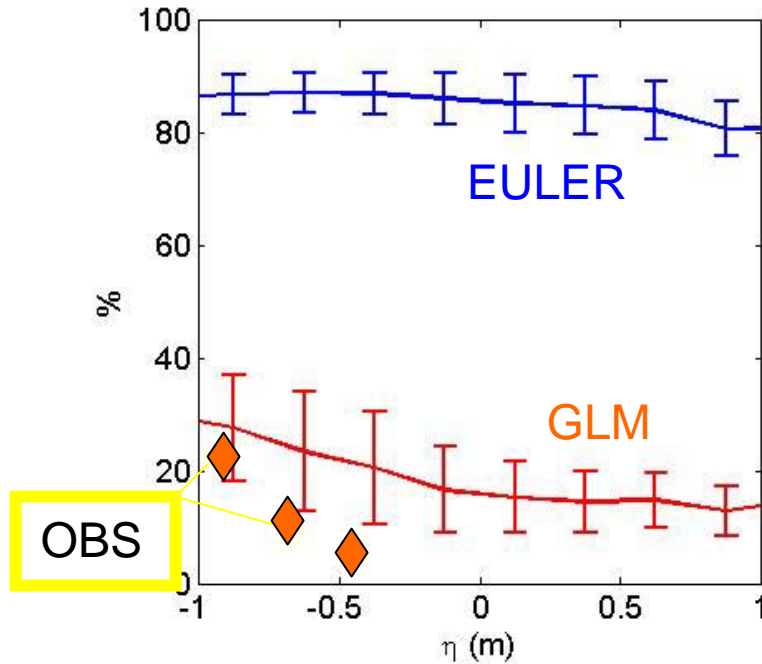
Figure 7 Estimated percentage of the mean hourly GLM (solid red line) and mean Eulerian (solid blue line) drifter exists for yeardays 124 through 126 as function of the tidal elevation plus or minus one standard deviation (denoted by the vertical bars). Observations of percentage drifter exits as function of tidal elevation indicated by green dots on yeardays 124, 125, 127 and 130 corresponding to times of normally incident waves during RCEX.

The resulting tidally-averaged retention rates, corresponding to the percentage of drifters retained in the surf zone within one hour are 0.82 for the GLM velocities and 0.15 for the Eulerian velocities (Figure 7). This corresponds to retention relaxation time scale of O(5) hours for the GLM velocities and less than 1 hour for the Eulerian velocities. As a result the retention time of floating surf zone material on a rip channeled beach is significantly longer than originally anticipated. This also holds for other suspended material such as sediment fines, algae, bubbles and other organic matter tracking the fluid motions,and are therefore subject to Stokes drift. However, their retention also depends on the vertical advection given the fact these agents are not confined to the water surface only and the GLM velocities vary with depth.

In summary, the model calculations closely match the rip-current surface flow field inferred from GPS-equipped drifter trajectories. Also the ADCP-observed temporal velocity variability over a period of three days with normally incident swell is reproduced by the computations, although the strong vertical attenuation of the sub-surface rip current velocities at the most offshore location is not well predicted. Seeding the surf zone with a large number of equally spaced virtual drifters the computed instantaneous surface velocity fields are used to calculate the drifter trajectories for the duration of an hour. Surfzone retention is examined by comparing the number of drifters that exit the surf zone compared to the total number of active drifters during one hour. Collecting the hourly drifter exits, good agreement with the observed surfzone retention is obtained provided that Stokes drift is accounted for in the modeling of the computed drifter trajectories. By including Stokes drift O(20)\%

12

of the drifters exit the surf zone within one hour. Without Stokes drift, the estimated number of drifter-exits is O(85)%, an order of magnitude larger than the O(10)% of exits for the field observations.

IMPACT/APPLICATIONS

Understanding Lagrangian rip current behavior is critical for beach safety, water quality, water clarity, nearshore mixing, and sediment, biological, and nutrient exchange. The detailed spatial maps of velocity and vorticy will increase our understanding of rip current dynamics. These new observations are evalauted with Delft3D. The inclusion of Stokes in the prediction of the fate of floating surface material is essential. This finding has important consequences for calculating the transport of surface drifters but also sediment fines, algae, bubbles and other organic matter and as a result will also impact the predictions of both water clarity and water qualitity.

REFERENCES

Battjes, J.A., (1975). Modeling of turbulence in the surf zone. *Proc. Symp. on Modeling Tech.*, San Francisco, 1050-1061. ASCE.

Brown, J.W., J. MacMahan, A. Reniers, and E. Thornton, (2008). Diffusivity on a Rip Channeled Beach, submitted to J. Geophys. Res.

Davis, R. E., (1991). Observing the general circulation with floats. Deep-Sea Res., 38, S531S571.

Inman, D. L., Tait, R. J., and Nordstrom, C. E., (1971). Mixing in the surfzone. *J. Geophysical Research.* **26**. 3493–3514.

Johnson, D., and Pattiaratchi, C., (2004). Transient rip currents and nearshore circulation on a swell-dominated beach. *J. Geophysical Research.* **109**.

MacMahan, J., J. Brown, and E.B. Thornton, Low-cost handheld Global Positioning Systems for measuring surf zone currents, *J. Coastal Res,* DOI: 10.2112/08-1000.1, 2008

MacMahan, J., J. Brown, A.J.H.M. Reniers, J. Brown, E.B. Thornton, T.P. Stanton and E. Gallagher, Lagrangian observations on a rip-channeled beach, submitted to *Geophysical Res. Letters*, 2008a.

Reniers, A., J. MacMahan, E. B. Thornton, and T. P. Stanton, Modeling of very low frequency motions during RIPEX, J. Geophys. Res., doi:10.1029/2005JC003122, 2007.

Spydell, M., Feddersen, F., Guza, R., and Schmidt, W., (2007). Observing surfzone dispersion with drifters. *J. Phys. Ocean.*, 37 (12). 2920-2939.

Swenson, M.S., and P. P. Niiler, (1996). Statistical analysis of the surface circulation of the California Current. J. of Geophy. Res. 101, 2263122645.

Talbot, M. M., and G. C. Bate, (1987). Rip current characteristics and their role in the exchange of water and surf diatoms between the surf zone and nearshore. Estuar. Coast. Shelf Sci. 25 (6). 707-720.

PUBLICATIONS

MacMahan, J., J. Brown, and E.B. Thornton, Low-cost handheld Global Positioning Systems for measuring surf zone currents, *J. Coastal Res,* DOI: 10.2112/08-1000.1, 2008

MacMahan, Jamie H., Thornton, Ed. B., Reniers, Ad. J.H.M., Stanton, Tim P., Symonds, Graham, Rip Currents Associated with Small Bathymetric Variations, *Marine Geology*, doi: 10.1016/j.margeo. 2008.08.006, 2008.

Brown, J.W., J. MacMahan, A. Reniers, and E. Thornton, Diffusivity on a Rip Channeled Beach, submitted to J. Geophys. Res, 2008.

MacMahan, J., J. Brown, A.J.H.M. Reniers, J. Brown, E.B. Thornton, T.P. Stanton and E. Gallagher, Lagrangian observations on a rip-channeled beach, submitted to *Geophysical Res. Letters*, 2008.

Reniers, A.J.H.M., J.H. MacMahan, E.B. Thornton, T.P. Stanton, M. Henriquez, J. Brown, J. Brown and E. Gallagher, Surfzone Retention on a Rip Channeled Beach, in preparation for *J. Geophys. Res*., 2008.

Reniers, A.J.H.M. and J.H. MacMahan, Rip Current Pulses, in preparation for *Geophysical Res. Letters*, 2008

PRESENTATIONS

Geiman, J. J. Kirby, A. Reniers, J. MacMahan, J. Brown, J. Brown, and T. Stanton, Wave-Averaged and wave-resolving simulations of the RCEX experiment: Mean flows and Drifter Dispersion, AGU Fall Meeting, 2008

Reniers, A. J. MacMahan, Surf zone Exchange on a Rip Channeled Beach, AGU Fall Meeting, 2008

Hendrickson, J. J. MacMahan, E. Thornton, M.Cook, T. Stanton, A. Reniers. Diurnal Cross-Shore Exchange on the Inner-Shelf in Southern Monterey Bay, CA, AGU Fall Meeting, 2008

J. Brown, J. MacMahan, A. Reniers, J. Brown, E. Thornton, T. Stanton, M. Orzech, Alongshore Sinuous Currents on a Rip-Channeled Beach, AGU Fall Meeting, 2008

Thornton, E., J. MacMahan, A. Reniers, J. Brown, T. Stanton, J. Brown, Rip Current Retention, AGU Fall Meeting, 2008

O' Neill, J. MacMahan, A. Reniers, E. Thornton, T. Stanton, J. Brown, Vertical Behavior of Rip Current Pulsations Outside the Surf Zone, AGU Fall Meeting, 2008

MacMahan, J., E. Thornton, T. Stanton, A. Reniers, J. Brown & J. Brown, Eulerian and Lagrangian measurements of rip currents during RCEX, ICCE 2008

Reniers A., J. MacMahan, E. Thornton, and T. Stanton, Modeling of 3D structure of rip current flows at RCEX, ICCE 2008

Kirby J.T., J. H. MacMahan, A. Reniers, J.Geiman, J. Brown, and T. Stanton, Model/Data Comparison for Lagrangian Trajectories and Mixing Estimates over Complex Nearshore Bathymetry, EuroMech Conference 2008.